J Mater Sci: Mater Med (2010) 21:557–565
DOI 10.1007/s10856-009-3880-4

Self-assembled particles of N-phthaloylchitosan-g-polycaprolactone molecular bottle brushes as carriers for controlled release of indometacin

Youju Huang · Liangbin Li · Yue'e Fang

Received: 24 June 2009 / Accepted: 17 September 2009 / Published online: 26 September 2009

Abstract A series of amphiphilic N-phthaloylchitosan-g-polycaprolactone molecular bottle brushes were prepared by "graft onto" method. The narrow distribution of polycaprolactone macromonomers ensures that the molecular bottle brushes can self-assemble into highly monodisperse particles, which have the ability to get a high loading efficiency of the hydrophobic drug, indometacin (INN). Searching for the effective drug loading ratio, three parameters such as polycaprolactone chain length, the grafting content and concentration of the molecular bottle brushes were tested to entrap INN. These encapsulated drug particles show sustained release of the encapsulated INN, of which 91.7% was released in 22 h at 37°C in phosphate buffered saline. The self-assembled particles of the molecular bottle brushes as carriers for INN can effectively prevent the drug from releasing quickly and prolong the release time, which is a promising candidate for potential clinical applications.

1 Introduction

Polymeric particles emerging as promising drug candidates have been received considerable interest in last decades [1–7]. Different molecular architectures such as block copolymers, star-shaped polymers, Y-shaped polymers, dendrimers and some proteins, peptides, peptidergic molecules have been designed to be drug carriers. However, it still remains as a challenging task for efficient drug delivery and targeting [8–16].

Polymeric particles formed by self-assembly have established themselves as effective drug carriers in potential clinical applications with a great success [17–20]. The self-assembled micelles possess a number of unbeatable advantages as potential carriers in the drug delivery system, which may resolve some critical problems of drugs such as poor solubility, tissue damage, unfavorable pharmacokinetics, poor biodistribution, etc. [21, 22]. Such aggregates have the ability to take drugs and to release them in aqueous solution. The hydrophobic groups serve as a micro reservoir for hydrophobic drugs and act as a depot to release drugs for a certain period of time, while hydrophilic chains reduce their interaction with plasma proteins and increase their half-life time in blood circulation. Since the drug carriers should be biodegradable, biocompatible and nontoxic, many investigations have been focused on the modification of natural hydrophilic biopolymers with hydrophobic biodegradable synthetic polymers [23].

In addition to the basic criterions such as biocompatibility and biodegradability, a good drug carrier requires a narrow distribution of particle size, the ability for higher drug encapsulation efficiency (EE) and other specific conditions. The narrow distribution of particle size ensures a well-controlled loading dose and a stable release process [24, 25]. Though macromolecular drug carriers are generally more robust than small molecular one, it is a big challenge to achieve a narrow size distribution for macromolecular carriers. As the unreasonably high quantities of the carrier can lead to problems of carrier toxicity,

Y. Huang · L. Li (✉)
National Synchrotron Radiation Lab and College of Nuclear Science and Technology, University of Science and Technology of China, Hefei 230026, People's Republic of China
e-mail: lbli@ustc.edu.cn

L. Li · Y. Fang
Department of Polymer Science and Engineering, University of Science and Technology of China, Hefei 230026, People's Republic of China

metabolism and elimination, a higher EE allows using lower drug carriers for the same amount of drugs [26, 27].

In this work, amphiphilic N-phthaloylchitosan-g-polycaprolactone (PHCS-g-PCL) molecular bottle brushes are designed to meet the requirements on narrow size distribution and high drug EE. Chitosan (CS) is a biodegradable polysaccharide extracted from crustacean shells, while polycaprolactone (PCL) is a biodegradable, biocompatible and flexible chain synthetic polymer. Both polymers have drawn increasing attention in drug and gene delivery system in recent years [28–40]. In order to achieve the narrow size distribution, PCL macromonomers, instead of monomers, are directly grafted onto phthalic anhydride modified CS (N-phthaloylchitosan, PHCS) main chain. This approach ensures a narrow distribution of PCL block length, which is the critical parameter controlling the size distribution of the self-assembled drug carriers. Searching for the effective drug loading ratio, PCL chain length, grafting content and the concentration of PHCS-g-PCL molecular bottle brushes are tested in this work. Results show that PHCS-g-PCL molecular bottle brushes self-assemble into particles with a narrow size distribution, which indeed give a high loading efficiency and stable drug release process. The drug-loaded nanoparticles have been widely used for nanoencapsulation, IV injection, combined cancer imaging and therapy, etc [41–43]. Combining the biodegradability and biocompatibility of the polymeric carriers and a high loading efficiency and stable drug release process of the drug-loaded nanoparticles, the encapsulated drug particles (INN-PHCS-g-PCL) are a promising candidate in clinical applications.

2 Experimental

2.1 Materials

Chitosan was obtained from San Huan Ocean Biochemical Co. Ltd. (Zhejiang, China). Its' degree of deacetylation and the molecular weight are 95% and 7.6×10^5, respectively. The PCLs terminated with hydroxyl groups with three different molecular weight (M_w = 1,250, 2,000 and 4,000, respectively) were purchased from SOLVAY, United Kingdom. Indometacin (INN) was purchased from Aldrich. 2,4-Tolylene diisocyanate (TDI), phthalic anhydride and hydrazine monohydrate were supplied by the First Reagent Factory of Shanghai (China). The CS and PCL were dried in vacuum oven at 50°C for 24 h prior to use. *N*,*N*-dimethylformamide (DMF) was distilled under reduced pressure from magnesium sulfate and stored over molecular sieves (4 Å). All other commercially available chemicals were used as received.

2.2 Synthesis of N-phthaloylchitosan-g-polycaprolactone bottle brushes

The PHCS-g-PCL molecular bottle brushes were prepared by "graft onto" method. The isocyano group terminated PCL macromonomers were prepared by previous literature [35, 44]. The PCL–NCO macromonomers were dissolved in anhydrous DMF in a 250 ml three-neck round-bottomed flask. The dried PHCS [45] solution with dibutyltin dilaurate as a catalyst in DMF was added in the three-neck round-bottomed flask. The reaction continued at 90°C for 3 h under stirring and a nitrogen atmosphere. The obtained product was poured into ice water and separated by filtration, extracted with acetone and dried in the vacuum oven at 80°C for 24 h. The schematic of grafting process and the final PHCS-g-PCL molecular bottle brushes structure were shown in Fig. 1a and b, respectively.

2.3 Self-assembly and drug loading

The self-assembled structures of PHCS-g-PCL molecular bottle brushes without and with the presence of INN were prepared by a dialysis method. Briefly, PHCS-g-PCL molecular bottle brushes (30 mg) were dissolved in 30 ml DMF. For drug loading, a predetermined amount of INN (20 mg) was added to the PHCS-g-PCL molecular bottle brushes solution. The solution was vigorously stirred for 2 h at room temperature and then dialyzed against water using a membrane with a molecular weight cut off ,7,000. The dialysis takes 2 days, during which PHCS-g-PCL molecular bottle brushes self-assembled into particles slowly. With the presence of INN, a portion of INN was encapsulated into the hydrophobic cores of PHCS-g-PCL particles, while some INN was precipitated out. In order to get ride of extra INN which are not encapsulated inside PHCS-g-PCL molecular bottle brushes, the final solution was filtered and washed with acetone three times. The total amounts of INN in the encapsulated drug particles (INN-PHCS-g-PCL) were calculated by a predetermined mount of INN-PHCS-g-PCL particles dissolved in the DMF detected at 320 nm using a UV–Vis detector (UV-2401PC). The drug loading capacity (LC) and encapsulation efficiency (EE) of PHCS-g-PCL were calculated by using Eqs. 1 and 2, respectively [46].

$$\mathrm{LC} = B/C \times 100 \quad (1)$$

$$\mathrm{EE} = B/A \times 100 \quad (2)$$

where A = total amount of added INN; B = total amount of INN in the INN-PHCS-g-PCL particles; C = weight of PHCS-g-PCL molecular bottle brushes.

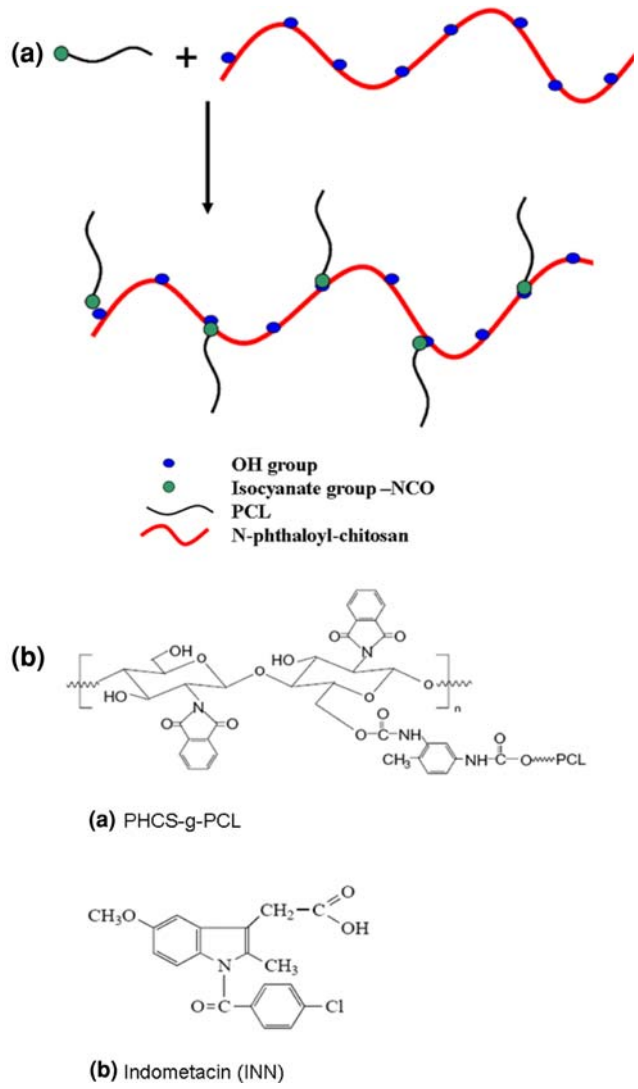

Fig. 1 **a** The schematic of graft process of PHCS-g-PCL molecular bottle brushes; **b** molecular structures of **a** final PHCS-g-PCL molecular bottle brushes and **b** INN

2.4 Particle size and morphology

The hydrodynamic diameters and diameter distribution of the self-assembled particles were measured using dynamic light scattering (DLS) carried out on a Malvern Zetasizer Nano ZS90 equipped with a He–Ne laser (633 nm), and 90° collecting optics. Malvern Dispersion Technology Software 4.20 was applied for data analysis. All measurements were carried out at 25°C. Micelles of PHCS-g-PCL molecular bottle brushes without and with the presence of INN were formed through a dialysis method. The obtained micelles of PHCS-g-PCL molecular bottle brushes without and with the presence of INN are highly stable, which could not transform into other states for months. Then, the micelles of PHCS-g-PCL molecular bottle brushes without and with the presence of INN were transferred into the sample cell of DLS to get the hydrodynamic diameters and diameter distribution of the self-assembled particles. The morphology was observed by H-800 transmission electron micrographs (TEM) and scanning electron microscopy (SEM) on the dried samples. Samples were performed as follows: a drop of sample solution was deposited on a copper grid coated first with a thin film of Formvar and then with carbon. The specimen was left to permit evaporation of water at atmospheric pressure for several minutes.

2.5 In vitro drug release

The dried PHCS-g-PCL particles (45 mg) encapsulating INN and 20 ml of phosphate buffered saline (PBS, 0.1 M, pH 7.4) were put into a dialysis bag (cut off molecular weight: 7,000). Then, the dialysis bag was introduced into a vial containing 200 ml of PBS. The systems were immersed in a thermostatic bath (37°C). At appropriate intervals, 3 ml samples of solution were withdrawn from the vials and assayed for drug release by UV spectrophotometer at 320 nm and replaced by 3 ml of fresh PBS.

3 Results and discussion

3.1 The synthesis and characterization of the graft polymers

It is more difficult for the higher M_n macromonomer chains to be incorporated into the macromolecule backbones because of chain translational diffusion limitations or trapping of terminal groups in large chain coils or both [47]. In order to facilitate the copolymerization of grafting hydrophobic PCL onto hydrophilic CS, PHCS, instead of CS was used. This approach makes copolymerization possible in a DMF homogeneous solution. The obtained one end enveloped PCL–NCO chains were grafted onto CS due to the reaction between OH groups from PHCS and the terminated NCO groups from PCL–NCO prepolymers in DMF homogeneous solution.

Compared the FTIR spectra of the PHCS-g-PCL molecular bottle brushes with that of PHCS (Fig. 2), a new peak at 1,538 cm^{-1} occurred in the spectra of the PHCS-g-PCL molecular bottle brushes. It is assigned as the absorbance of amide ester linkage (–OCONH–). Stronger absorbance at 2,800–3,000 cm^{-1} for ν_{C-H} (of CH_2) implied the successful introduction of the PCL chains. The ^{1}H-NMR spectra of the PHCS-g-PCL copolymer in Fig. 3 also confirmed that the PCL chains were grafted onto PHCS. The peaks at 2.5 ppm belong to the solvent DMSO-d_6. The strong signals originated from the PCL side chain are detected at 1.2 ppm ($CH_2CH_2C\mathbf{H}_2$–CH_2CH_2), 1.50 ppm ($CH_2C\mathbf{H}_2CH_2C\mathbf{H}_2CH_2$), 2.24 ppm ($COC\mathbf{H}_2$) and

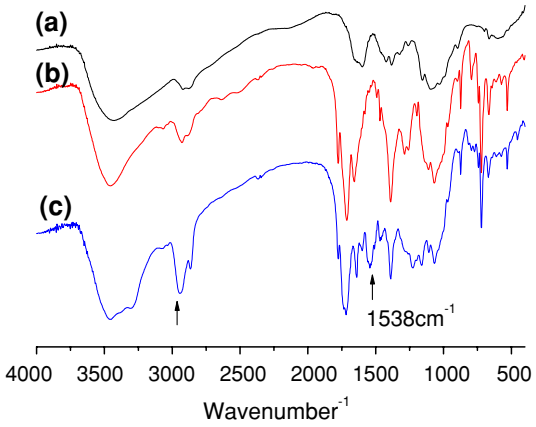

Fig. 2 FT-IR spectra of chitosan (**a**), PHCS (**b**), PHCS-graft-PCL molecular bottle brushes (**c**)

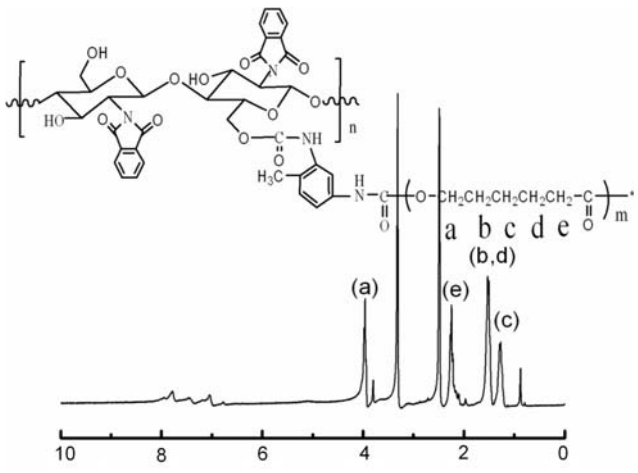

Fig. 3 ^{1}H-NMR spectrum of PHCS-g-PCL molecular bottle brushes

3.95 ppm (C**H**$_2$O), respectively, while the broad peaks of CS backbone hydrogens are at 2.8–4.0 ppm. The peak at 0.9 ppm is OH groups of CS. Aromatic phthalimido peaks at 7.0–8.0 ppm are associated with phenyl ring of TDI and phthalic anhydride.

The weight of the grafted macromonomer cannot be measured directly. However, it can be estimated from the measured weight of the original and residual samples. The grafting content ($G\%$) was calculated as follows:

$$G\% = (W_g - W_0)/W_0 \times 100,$$

where W_g, W_0 are the weight of PHCS-g-PCL molecular bottle brushes and PHCS, respectively.

We also calculated the degree of PCL substitution and the average number of PCL side chains per units of PHCS with following equations:

Table 1 The detail results of all samples

Sample	PCL side chain (M_w)	G (%)	N	DS
1	1,250	78.3	92	0.182
2	2,000	80.6	59	0.117
3	4,000	76.2	28	0.055
4	2,000	65.1	47	0.095
5	2,000	117.5	86	0.171
6	2,000	91.3	67	0.133

$$\mathrm{DS_{PCL}} = \frac{m \times G\%/M_{\mathrm{PCL}}}{m/M_{\mathrm{PHCS'unit}}} \qquad N = \frac{m \times G\%/M_{\mathrm{PCL}}}{m/M_{\mathrm{PHCS}}}$$

where $\mathrm{DS_{PCL}}$ is the substitution degree of the PCL at hydroxyl sites, N is the average number of PCL side chains per units of PHCS and m is the supposed weight of PHCS. The detailed results of all samples are listed in the Table 1. This defines the structure and molecular properties of the PHCS-g-PCL molecular bottle brushes.

3.2 Self-assembly without and with INN drug

The hydrodynamic diameters and diameter distribution of the self-assembled spherical particles without and with the presence of INN drug were measured with a Zeta Sizer (Nano-ZS90) at a temperature of 25°C. Figure 4 shows a representative result from a sample grafted PCL with a molecular weight of 2,000 and grafting content of 91.1%. Without the presence of INN, PHCS-g-PCL conjugates forms particles with an average diameter of 320 nm and a narrow size distribution in aqueous solution (Fig. 4a). The presence of INN (10^{-2} g/ml) leads to an increase of particle size to 460 nm (Fig. 4b), while the distribution of

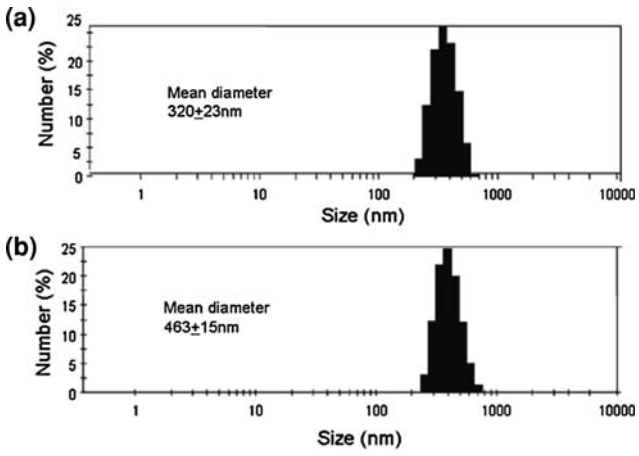

Fig. 4 Size of the PHCS-g-PCL particles (**a**) and the INN-PHCS-g-PCL particles (**b**) mean diameter in pure water

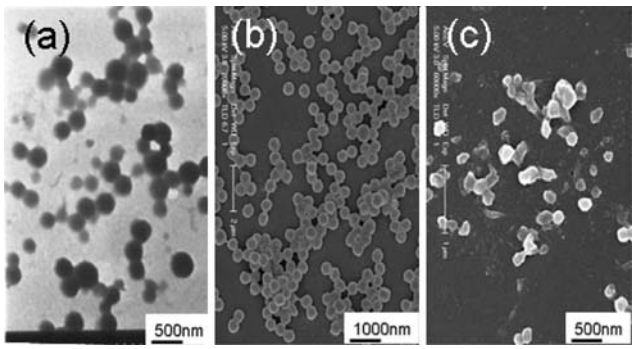

Fig. 5 TEM (**a**) and SEM (**b**) of the PHCS-g-PCL particles and INN-PHCS-g-PCL particles (**c**)

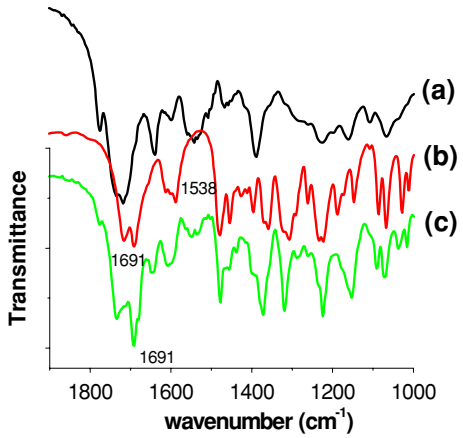

Fig. 6 IR spectra: **a** PHCS-g-PCL; **b** INN; **c** INN-loaded PHCS-g-PCL

particle size remains narrow. The increase of particle size by INN suggests that PHCS-g-PCL entraps INN molecules partly in its hydrophobic inner cores and partly in the PHCS shell because of the interaction of hydrophobic phthaloyl groups with drugs.

The morphology of PHCS-g-PCL molecular bottle brushes was observed by the SEM and TEM as shown in Fig. 5, which was obtained from the same samples as for Fig. 4. Without the presence of INN, PHCS-g-PCL molecular bottle brushes self-assemble into spherical particles with a diameter of around 320 nm (Fig. 5a and b), which is the same as that measured with Zeta Sizer. The presence of INN deforms the shape of the particles from spherical to an irregular morphological feature (Fig. 5c). Compared results from Zeta Sizer, INN-PHCS-g-PCL particles measured with SEM are significantly smaller. Because samples for SEM measurements are dried, a contraction induced by drying seems normal. Nevertheless, compared the nearly identical size of PHCS-g-PCL particles measured with SEM and Zeta Sizer, the contraction of INN-PHCS-g-PCL particles reveals INN leads to an entrapping of water in the particles. INN has a carboxyl group and a carbonyl group, which can interact with water molecules by hydrogen bonding. In the drug loading process, the PHCS-g-PCL molecular bottle brushes easily incorporate the drug and water molecules interacted with drug by hydrogen bonding in the nanoparticles. The contraction of INN-PHCS-g-PCL particles may be partly responsible for the irregular shape of the dried particles observed with SEM.

3.3 Infrared analysis of INN-PHCS-g-PCL particles

The encapsulation of INN in PHCS-g-PCL molecular bottle brushes is further checked with FTIR, which is given in Fig. 6. The PHCS-g-PCL molecular bottle brushes (Fig. 6a) shows a distinct primary amide ester linkage (–OCONH–) vibration at 1,538 cm^{-1} which confirmed the successful grafting of the PCL chains. Pure INN (Fig. 6b) shows strong absorption of the carbonyl group at 1,691 cm^{-1}. The absorption peak at 1,691 cm^{-1} was observed on the INN-PHCS-g-PCL self-assembled particles (Fig. 6c). Evidently, INN is encapsulated in PHCS-g-PCL particles.

3.4 Drug encapsulation efficiency and loading capacity of PHCS-g-PCL molecular bottle brushes

The relationship between three parameters (PCL molecular weight, grafting content and concentration of PHCS-g-PCL molecular bottle brushes) and EE or LC were investigated and the results were summarized in Table 2. It seems that a variation of PCL molecular weight from 1,250 to 4,000 does not change the EE, while the EE and the LC show strong correlation with the grafting content and the concentration of PHCS-g-PCL molecular bottle brushes (C_{cop}).

Figure 7a and b plots the EE versus the grafting content and the copolymer concentration C_{cop}, respectively. The PCL macromonomers have a molecular weight of 2,000. After a flat region below a grafting content of 80%, the EE increases nearly linearly with the increase of the grafting content. As INN is hydrophobic, which is prone to locate in PCL region, a higher grafted PCL corresponding to a higher encapsulated INN is logical. Keeping a constant ratio of 1.5 between the concentrations of the PHCS-g-PCL copolymer and drug INN, increasing their concentration C_{cop} and C_{INN} leads to a significant increase of the EE, which is linearly correlated with each other with a slope of about 2.98%/10^{-3}g/ml. Thus a further increase of the EE may be achieved with higher concentrations of copolymer and INN. For example, keeping the ratio between the copolymer and the drug constant, a EE of 50% may be obtained in a solution with a copolymer concentration of about 13×10^{-3} g/ml.

Table 2 Influence of the molecular weight of PCL side chain, the grafting content of PCL side chain (%) and the copolymer concentration (C_{cop}) (10^{-3} g/ml) on the EE and the LC

Sample	PCL side chain (M_W)	G (%)	(C_{cop}) 10^{-3} g/ml	PHCS-g-PCL/ INN (wt/wt)	EE (%)	LC (%)
1	1,250	78.3	1.0	1.5	9.25	6.20
2	2,000	80.6	1.0	1.5	8.90	5.96
3	4,000	76.2	1.0	1.5	9.10	6.10
4	2,000	65.1	1.0	1.5	8.57	5.74
5	2,000	117.5	1.0	1.5	13.10	8.78
6	2,000	91.3	0.1	1.5	9.20	6.16
7	2,000	91.3	1.0	1.5	12.50	8.37
8	2,000	91.3	5.0	1.5	23.70	15.88
9	2,000	91.3	10	1.5	39.00	26.13

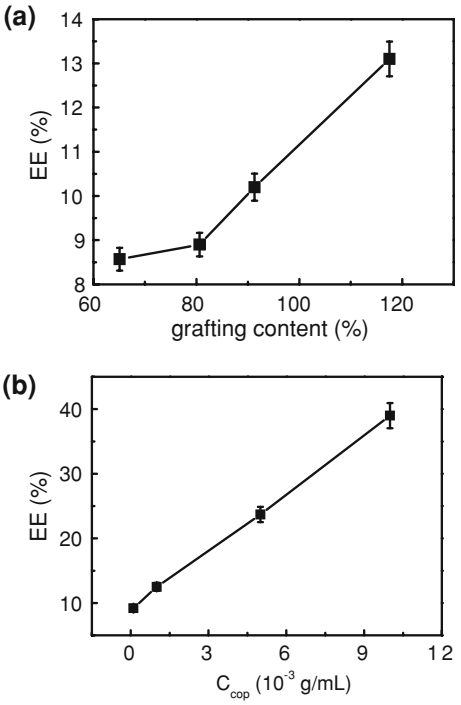

Fig. 7 Influence of the grafting content of PCL side chain (%) and the copolymer concentration (C_{cop}) (10^{-3} g/ml) on the EE

3.5 Release of INN from PHCS-g-PCL molecular bottle brushes

Figure 8 shows the release profiles of INN from INN-PHCS-g-PCL particles in PBS (pH = 7.4) at 37°C. In contrast to the rapid release of the free drug from a cellulose membrane (97% release in 5 h), the drug release from the PHCS-g-PCL particles is slowed down. Nearly 90% of the loaded INN is released from INN-PHCS-g-PCL particles in 22 h. An initial burst release followed by a slowly sustained release of INN occurs in the INN-PHCS-g-PCL particles.

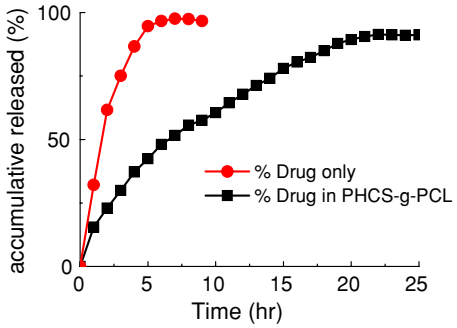

Fig. 8 In vitro release profile of INN from the PHCS-g-PCL particles

4 Discussion

The strategy of using PCL macromonomers instead of monomers in the grafting shows a clear advantage to obtain self-assembled particles with narrow size distribution. Grafting with macromonomers, the total molecular weight are not only determined by the grafting content, but also controlled by the PCL molecular weight. With a PCL macromonomers with a nearly mono-dispersing molecular weight, grafting content is the only parameters that affect the molecular weight of PHCS-g-PCL molecular bottle brushes copolymer, which can be tuned through reaction time. Above the critical concentration, it is a natural result that the hydrophobic PCL side chains and hydrophilic CS main chain micro-phase separates in aqueous environment and self-assembles into particles. The size of the self-assembled particles is much larger than the radius of gyration R_G of single polymers (see Figs. 4, 5). With a rough estimation, a particle with a diameter of 320 nm contains about 50 copolymer chains. The hydrophobicity of the building blocks and the interfacial free energy with water make such a choice of particle size [48].

We also made effort to study the self-assembly behavior of chitosan-g-PCL (CS-g-PCL) copolymer (the phthaloyl groups deprotected from PCL-g-PHCS). Unfortunately,

under similar condition employed on PHCS-g-PCL molecular bottle brushes, no particles were obtained. The CS-g-PCL molecular bottle brushes coagulated and formed membrane on the copper grid rather than self-assembled into spherical particles, possibly because of the strong intra- and inter-hydrogen bonds between amino groups of CS and other groups, e.g., hydroxyl groups. Thus, the drugs loading experiments were only studied with the PHCS-g-PCL molecular bottle brushes particles as carriers. Polymer brushes have unique physical and chemical properties arising from their regular multibranched structure and long aspect ratios, which have been widely used for bioelectronic applications, immunosensors, drug carriers, etc. [49–51]. In our research, the novel well-designed amphiphilic polymer brushes are a biodegradable, biocompatible and flexible chain synthetic polymer, which is a promising drug carrier candidate in clinical applications.

From weight and FTIR measurements, it is no doubt that INN drug molecules are encapsulated inside the particles. A schematic drawing is shown in Fig. 9 to illustrate the mechanism. As INN is a hydrophobic drug, it should be prone to locate inside PCL regions. This is also supported by the correlation between grafting content and EE or LC. Above certain grafting content, the EE and the LC increase almost linearly with the grafting content (see Table 2 and Fig. 7a). Evidently, PCL side chains in the molecular bottle brushes play an important role at the drug encapsulation. The molecular weight of the grafted PCL macromonomers seems not affect the EE significantly. As the PCL content instead of the individual chain length determines the EE, it is a natural result that the variation of molecular weight of PCL did not affect the EE obviously, provided a nearly identical grafting content for those samples (see Table 2, Samples 1–3).

It is surprising that the EE increases linearly with the increase of the concentrations of copolymer and drug INN, though the ratio between them remains constant (see Fig. 7b). Taking the interaction between PCL and drug INN alone is not possible to explain this phenomenon. Here, we are dealing with a three-phase system and one has to take into account the solvent effect and the kinetics of self-assembly. During dialysis, PHCS-g-PCL molecular bottle brushes can self-assemble without and with the encapsulation of INN, while INN can either precipitate or join in the self-assembled particles. Increasing the concentrations of INN and PHCS-g-PCL molecular bottle brushes provides a higher probability for PHCS-g-PCL to catch INN during the self-assembly process, though their concentration ratio remains constant. Evidently, the drug loading process is not only controlled by thermodynamic driving force, but also strongly affected by kinetic competition. This is also supported by the irregular shape of the particles with drug loaded, compared with that without the presence of drug. Without the presence of drug, the kinetic effect during the self-assembly of PHCS-g-PCL molecular bottle brushes is much weaker, which leads to the uniform size and spherical shape. The presence of drug introduces more parameters, such as the amount and the location of drug inside the particles, and more kinetic competitions, which leads to the irregular shape of particles. Our results demonstrate not only molecular structure, but also solvent quality and self-assembling process can control the EE and final morphology, which are essential criterions for drug carriers.

It is important to point out that the drug EE and LC of the PHCS-g-PCL molecular bottle brushes are relatively high (39% and 26.1%, respectively), which is higher than that of many traditional micelles [52]. These improved properties are attributed to their regular multibranched structure of the PHCS-g-PCL molecular bottle brushes as well as the strong interactions between the drug and the PHCS-g-PCL molecular bottle brushes. Carbonyl groups and hydroxyl groups in the PHCS-g-PCL molecular bottle brushes have strong hydrogen-bonding interactions with the carboxyl group of INN. These interactions might effectively improve the EE of PHCS-g-PCL molecular bottle brushes and protect the drug from releasing quickly and prolong the drug release time.

In contrast to the rapid release of the free drug from a cellulose membrane (97% release in 5 h), the drug release from the PHCS-g-PCL particles was slowed down (Fig. 9). The release pattern of INN from PHCS-g-PCL particles has two different stages. The first stage is in about 5 h, where the amount of the released drug versus time has a higher slope than that of the second stage. Forty percentage loaded drug was released during this period. The first stage of the drug release is always involving in the drugs which were

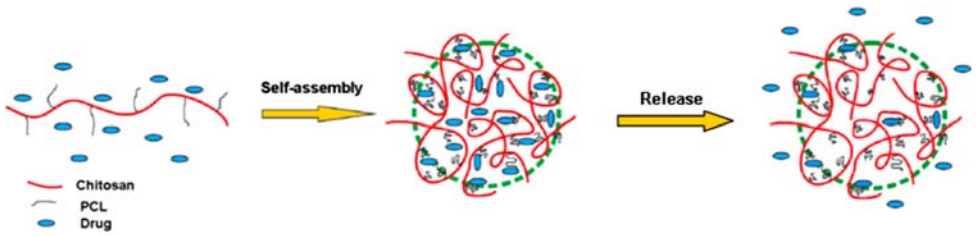

Fig. 9 Schematic illustration of the drug encapsulation and release

loaded in the PHCS shell because of interaction of hydrogen bonds with drugs, which escape fast at the beginning. At the second stage, the slowdown of the release is due to lower concentration inside the drug carrier and stronger drug–carrier interactions in the PCL core. It takes about 17 h to release the rest 50% drugs in the second stage. This confirmed that PHCS-g-PCL molecular bottle brushes as carriers can protect the drug from releasing quickly and prolong the drug release time. Combining the biodegradability and biocompatibility of the polymeric carriers, the high loading efficiency and the stable drug release process, the particles with encapsulated drug (INN-PHCS-g-PCL) is a promising candidate in the potential clinical applications. For example, the PHCS-g-PCL molecular bottle brushes can incorporate some curative hydrophobic drug molecules to form nanoencapsulation for oral administration or to prepare the stable micelle in the aqueous solution for IV injection.

5 Conclusion

In this study, amphiphilic PHCS-g-PCL molecular bottle brushes were prepared by "graft onto" method. The unique properties arising from their regular multibranched structure have the ability to get a high loading efficiency (up to 26.1 wt%) of hydrophobic drug, INN. Three parameters such as PCL chain length, grafting content and the concentration of molecular bottle brushes were searched to entrap the drug. These particles with encapsulated drug showed sustained release of INN, of which 91.7% was released in 22 h at 37°C in phosphate buffered saline. The self-assembled particles of PHCS-g-PCL molecular bottle brushes as carriers for INN can effectively protect the drug from releasing quickly and prolong the drug release time. Combining the biodegradability and biocompatibility of the polymeric carriers, the high loading efficiency and the stable drug release process, the drug-loaded nanoparticles (INN-PHCS-g-PCL) are a promising candidate in the potential clinical applications.

Acknowledgement The authors thank the National Natural Science Foundation of China (No. 50573073) for financial support of this research.

References

1. Pasut G, Veronese FM. Polymer–drug conjugation, recent achievements and general strategies. Progr Polym Sci. 2007;32:933–61.
2. Li C, Wallace S. Polymer-drug conjugates: recent development in clinical oncology. Adv Drug Deliv Rev. 2008;60:886–98.
3. Wang AH, Tao C, Cui Y, Duan L, Yang Y, Li J. Assembly of environmental sensitive microcapsules of PNIPAAm and alginate acid and their application in drug release. J Colloid Interface Sci. 2009;332:271–9.
4. Talelli M, Rijcken CJF, Lammers T, Seevinck PR, Storm G, Nostrum CF, et al. Superparamagnetic iron oxide nanoparticles encapsulated in biodegradable thermosensitive polymeric micelles: toward a targeted nanomedicine suitable for image-guided drug delivery. Langmuir. 2009;25:2060–7.
5. Lue SJ, Hsu JJ, Wei TC. Drug permeation modeling through the thermo-sensitive membranes of poly (*N*-isopropylacrylamide) brushes grafted onto micro-porous films. J Membr Sci. 2008;321:146–54.
6. Prabaharan M, Grailer JJ, Steeber DA, Gong SQ. Stimuli-responsive chitosan-graft-poly (*N*-vinylcaprolactam) as a promising material for controlled hydrophobic drug delivery. Macromol Biosci. 2008;8:843–51.
7. Nystrom AM, Xu ZQ, Xu JQ, Taylor S, Nittis T, Stewart SA, et al. SCKs as nanoparticle carriers of doxorubicin: investigation of core composition on the loading, release and cytotoxicity profiles. Chem. Commun. 2008;30:3579–81.
8. Du J, Sun R, Zhang S, Zhang LF, Xiong CD, Peng YX. Novel polyelectrolyte carboxymethyl konjac glucomannan–chitosan nanoparticles for drug delivery. I. Physicochemical characterization of the carboxymethyl konjac glucomannan-chitosan nanoparticles. Biopolymers. 2005;78:1–8.
9. Brovarone V, Baino F, Miola M, Mortera R, Onida B, Verné E. Glass–ceramic scaffolds containing silica mesophases for bone grafting and drug delivery. J Mater Sci: Mater Med. 2009;20:809–20.
10. Liu YF, Huang KL, Peng DM, Liu SQ, Wu H. Preparation of poly (butylene-co-epsilon-caprolactone carbonate) and their use as drug carriers for a controlled delivery system. J Polym Sci A Polym Chem. 2007;45:2152–60.
11. Mezo G, Kajtar J, Nagy I, Szekerke M, Hudecz F. Carrier design: synthesis and conformational studies of poly (L-lysine) based branched polypeptides with hydroxyl groups in the side chains. Biopolymers. 1997;42:719–30.
12. Sood A, Panchagnula R. Peroral route: an opportunity for protein and peptide drug delivery. Chem Rev. 2001;101:3275–303.
13. Njikang GN, Gauthier M, Li J. Sustained release properties of arborescent polystyrene-graft-poly (2-vinylpyridine) copolymers. Polymer. 2008;49:5474–81.
14. Gao C, Xu YM, Yan DY, Chen W. Water-soluble degradable hyperbranched polyesters: novel candidates for drug delivery? Biomacromolecules. 2003;4:704–12.
15. Li X, Wu Q, Chen ZC, Gong XG, Lin XF. Preparation, characterization and controlled release of liver-targeting nanoparticles from the amphiphilic random copolymer. Polymer. 2008;49:4769–75.
16. Sen G, Pal S. Microwave initiated synthesis of polyacrylamide grafted carboxymethylstarch (CMS-g-PAM): application as a novel matrix for sustained drug release. Int J Biol Macromol. 2009;45:48–55.
17. Rosler A, Vandermeulen GWM, Klok HA. Advanced drug delivery devices via self-assembly of amphiphilic block copolymers. Adv Drug Deliv Rev. 2001;53:95–108.
18. Torchilin VP. Structure and design of polymeric surfactant-based drug delivery systems. J. Controlled Release. 2001;73:137–72.
19. Haag R. Supramolecular drug-delivery systems based on polymeric core–shell architectures. Angew Chem Int Ed. 2004;43:278–82.
20. Soppimath KS. Biodegradable polymeric nanoparticles as drug delivery devices. J. Controlled Release. 2001;70:1–20.
21. Miguel S, Limer AJ, Haddleton DM, Catalina F, Peinado C. Biodegradable and thermoresponsive micelles of triblock copolymers based on 2-(*N*,*N*-dimethylamino) ethyl methacrylate and epsilon-caprolactone for controlled drug delivery. Eur Polym J. 2008;44:3853–63.

22. Allen TM, Cullis PR. Drug delivery systems: entering the mainstream. Science. 2004;303:1818–22.
23. Janes KA, Calvo P, Alonso MJ. Polysaccharide colloidal particles as delivery systems for macromolecules. Adv Drug Deliv Rev. 2001;47:83–97.
24. Berkland C, King M, Cox A, Kim K, Pack DW. Precise control of PLG microsphere size provides enhanced control of drug release rate. J Controlled Release. 2002;82:137–47.
25. Zhang H, Oh M, Allen C, Kumacheva E. Monodisperse chitosan nanoparticles for mucosal drug delivery. Biomacromolecules. 2004;5:2461–8.
26. Ross BP, Braddy AC, McGeary RP, Blanchfield JT, Prokai L, Toth I. Micellar aggregation and membrane partitioning of bile salts, fatty acids, sodium dodecyl sulfate, and sugar-conjugated fatty acids: correlation with hemolytic potency and implications for drug delivery. Mol Pharmaceut. 2004;1:233–45.
27. Sha J, Ye K. Nanoparticle-mediated drug delivery and gene therapy. Biotechnol Prog. 2007;23:32–41.
28. Kim TH, Jiang HL, Jere D, Park IK, Cho MH, Nah JW, et al. Chemical modification of chitosan as a gene carrier in vitro and in vivo. Prog Polym Sci. 2007;32:726–53.
29. Kumar MNVR, Muzzarelli RAA, Muzzarelli C, Sashiwa H, Domb AJ. Chitosan chemistry and pharmaceutical perspectives. Chem Rev. 2004;104:6017–84.
30. Mourya VK, Inamdar NN. Trimethyl chitosan and its applications in drug delivery. J Mater Sci: Mater Med. 2009;20:1057–79.
31. Kim K, Kwon S, Park JH, Chung H, Jeong SY, Kwon IC, et al. Physicochemical characterizations of self-assembled nanoparticles of glycol chitosan-deoxycholic acd conjugates. Biomacromolecules. 2005;6:1154–8.
32. Soo PL, Luo L, Maysinger D, Eisenberg A. Incorporation and release of hydrophobic probes in biocompatible polycaprolactone-block-poly (ethylene oxide) micelles: implications for drug delivery. Langmuir. 2002;18:9996–10004.
33. Qian F, Cui F, Ding J, Tang C, Yin C. Chitosan graft copolymer nanoparticles for oral protein drug delivery: preparation and characterization. Biomacromolecules. 2006;7:2722–7.
34. Bodnar M, Hartmann JF, Borbely J. Synthesis and study of cross-linked chitosan-*N*-poly (ethylene glycol) nanoparticles. Biomacromolecules. 2006;7:3030–6.
35. Huang YJ, Li LB, Fang Y. Preparation of size-tunable, highly monodisperse particles by self-assembly of N-phthaloylchitosan-g-polycaprolactone molecular bottle brushes. Mater Lett. 2009; 63:1416–8.
36. Holappa J, Nevalainen T, Soininen P, Elomaa M, Safin R, Másson M, et al. *N*-chloroacyl-6-*O*-triphenylmethylchitosans: useful intermediates for synthetic modifications of chitosan. Biomacromolecules. 2005;6:858–63.
37. Fernandez-Megia E, Novoa-Carballal R, Quiñoá E, Riguera R. Conjugation of bioactive ligands to PEG-grafted chitosan at the distal end of PEG. Biomacromolecules. 2007;8:833–42.
38. Panyam J, Williams D, Dash A, Leslie-Pelecky D, Labhasetwar V. Solid-state solubility influences encapsulation and release of hydrophobic drugs from PLGA/PLA nanoparticles. J Pharm Sci. 2004;93:1804–14.
39. Diez-Sales O, Dolz M, Hernsndez MJ, Casanovas A, Herraez M. Acyclovir delivery matrices based on poly (ethylene glycol)/chitosan semi-interpenetrating networks. J Pharm Sci. 2007;96:1653–7.
40. Zheng YL, Wu Y, Yang WL, Wang CC, Fu SK, Shen XZ. Preparation, characterization, and drug release in vitro of chitosan-glycyrrhetic acid nanoparticles. J Pharm Sci. 2006;95:181–91.
41. Story C. A new method for preventing restenosis: a single IV injection of drug-loaded nanoparticles. J Controlled Release. 2009;133:87.
42. Yu MK, Jeong YY, Park J, Park S, Kim JW, Min JJ, et al. Drug-loaded superparamagnetic iron oxide nanoparticles for combined cancer imaging and therapy in vivo. Angew Chem Int Ed. 2008;47:5362–5.
43. Reis CP, Neufeld RJ, Ribeiro AJ, Veiga F. Nanoencapsulation I. Methods for preparation of drug-loaded polymeric nanoparticles. Nanomedicine. 2006;2:8–21.
44. Liu L, Li Y, Fang Y. Synthesis and characterization of chitosan-graft-polycaprolactone copolymers. Eur Polym J. 2004;40:2739–44.
45. Kurita K, Ikeda H, Yoshida Y, Shimojoh M, Harata M. Chemoselective protection of the amino groups of chitosan by controlled phthaloylation: facile preparation of a precursor useful for chemical modifications. Biomacromolecules. 2002;3:1–4.
46. Gupta KC, Ravkumar MNV. pH dependent hydrolysis and drug release behavior of chitosan/poly (ethylene glycol) polymer network microspheres. J Mater Sci: Mater Med. 2001;12:753–9.
47. Kolodka E, Wang WJ, Zhu SP, Hamielec AE. Copolymerization of propylene with poly (ethylene-*co*-propylene) macromonomer and branch chain-length dependence of rheological properties. Macromolecules. 2002;35:10062–70.
48. Forster S, Hermsdorf N, Bottcher C, Lindner P. Structure of polyelectrolyte block copolymer micelles. Macromolecules. 2002;35:4096–105.
49. Tam TK, Ornatska M, Pita M, Minko S, Katz E. Polymer brush-modified electrode with switchable and tunable redox activity for bioelectronic applications. J Phys Chem C. 2008;112:8438–45.
50. Kurosawaa S, Aizawaa H, Taliba ZA, Atthoffa B, Hilborne J. Synthesis of tethered-polymer brush by atom transfer radical polymerization from a plasma-polymerized-film-coated quartz crystal microbalance and its application for immunosensors. Biosens Bioelectron. 2004;20:1165–76.
51. Sato A, Cho SW, Hirai M, Yamayoshi A, Moriyama R, Yamano T, et al. Polymer brush-stabilized polyplex for a siRNA carrier with long circulatory half-life. J Controlled Release. 2007;122: 209–16.
52. Soppimath KS, Tan DCW, Yang YY. pH-triggered thermally responsive polymer core–shell nanoparticles for drug delivery. Adv Mater. 2005;17:318–23.